IET Nanobiotechnology

Research Article

IET Journals
The Institution of Engineering and Technology

Biologically-synthesised ZnO/CuO/Ag nanocomposite using propolis extract and coated on the gauze for wound healing applications

ISSN 1751-8741
Received on 27th January 2020
Revised 1st April 2020
Accepted on 14th April 2020
E-First on 21st July 2020
doi: 10.1049/iet-nbt.2020.0024
www.ietdl.org

Mahdi Bayrami[1], Abolfazl Bayrami[1] ✉, Aziz Habibi-Yangjeh[2], Mohammad Saleh Shafeeyan[3], Solmaz Feizpoor[2], Farid Mohammadi Arvanagh[1], Mohammad Reza Nourani[4], Ramezan Ali Taheri[4]

[1]*Department of Biology, Faculty of Science, University of Mohaghegh Ardabili, Ardabil, Iran*
[2]*Department of Chemistry, Faculty of Science, University of Mohaghegh Ardabili, Ardabil, Iran*
[3]*Department of Chemical Engineering, Faculty of Engineering, Golestan University, Aliabad Katoul, Iran*
[4]*Nanobiotechnology Research Center, Baqiyatallah University of Medical Sciences, Tehran, Iran*
✉ *E-mail: a_bayrami@uma.ac.ir*

Abstract: Wound healing has long been recognised as a major clinical challenge for which stablishing more effective wound therapies is necessary. The generation of metallic nanocomposites using biological compounds is emerging as a new promising strategy for this purpose. In this study, four metallic nanoparticles (NPs) with propolis extract (Ext) and one without propolis including ZnO/Ext, ZnO/Ag/Ext, ZnO/CuO/Ext, ZnO/Ag/CuO/Ext and ZnO/W were prepared by microwave method and assessed for their wound healing activity on excision experimental model of wounds in rats. The developed nanocomposites have been characterised by physico-chemical methods such as X-ray diffraction, scanning electron microscopy, diffuse reflectance UV–vis spectroscopy, Fourier transform infrared spectroscopy, thermogravimetric analysis and Brunauer–Emmett–Teller analyses. The wounded animals treated with the NPs/Ext in five groups for 18 days. Every 6 days, for measuring wound closure rate, three samples of each group were examined for histopathological analysis. The prepared tissue sections were investigated by haematoxylin and Eosin stainings for the formation of epidermis, dermis and muscular and Masson's trichrome staining for the formation of collagen fibres. These findings toughly support the probability of using this new ZnO/Ag/Ext materials dressing for a wound care performance with significant effect compared to other NPs.

1 Introduction

The skin has three major functions: protection, regulation and sensory perception. It acts as a barrier between the body and the external environment, protecting the body's organs and tissues against toxic chemicals, mechanical and microbial damage. When this barrier is breached as a result of physical trauma, chemical penetration or radiation, this protective function is lost, enabling the diffusion of microorganisms and pathogens into the underlying tissues leading to wound infections and other dermatological complications [1]. The majority of infections are dominated by pathogenic bacteria such as *Escherichia coli* and *Staphylococcus aureus* [2].

As soon as the skin is wounded, a sequence of complex physiological events, namely wound healing, are initiated to repair the damage and assure wound closure. Well-regulated immune responses to tissue injury taking place in a few overlapping stages aimed at reconstructing and repairing defected tissues and cells in vivo [3]. However, wound care treatment is an important area to be focused on since infections may result in exudate formation, dysregulated collagen deposition and wound healing postponing. Also, excess dehydration may disrupt the wet environment of the wound surface, leading to a delayed wound healing process [4]. Thus, understanding the general mechanism of wound healing activity in response to various types of dermal wound repair is of fundamental importance for developing efficient therapeutic strategies capable of stimulating the wound healing [5].

Nowadays, scientists have concentrated on the expansion of nanotechnology-based drug delivery systems, which offer promising prospects for delivering the desired quantity of the drugs into target sites, in addition to cell penetration efficiency. In this respect, metallic nanoparticles (NPs) have received a great deal of interest among researchers as they offer a number of attractive characteristics, such as lower toxicity, high surface-to-volume ratio and super-durability [6, 7]. Recent developments have demonstrated that zinc oxide NPs (ZnONPs) are promising candidates due to their potential to produce reactive oxygen species (ROSs), which show a major role in biological systems. The presence of ROSs may prohibit bacterial breeding and promote the wound healing process by improved cell adhesion and migration through stimulating growth factor-mediated pathway [8]. In addition, the bactericidal activity of silver NPs (AgNPs) on gram-positive and gram-negative bacteria (*Staphylococcus aureus* and *Escherichia coli*) has been extensively documented by many scientists and appears to be another effective therapy against multidrug-resisting bacteria [9]. Besides antimicrobial activity, silver-based NPs have anti-inflammatory characteristics that may be useful in maintaining proper moisture balance in the infected wounds [10]. There has been reported that Cu-containing NPs can also promote angiogenesis and contribute to accelerating wound healing, thereby stimulating the production of VEGF (vascular endothelial growth factor) and increasing the integrin activation level. Furthermore, copper NPs (CuNPs) may assist in early wound repair through enhancing collagen and fibrinogen formation, upregulating cell proliferation and migration, as well as inducing the generation of extracellular matrix polysaccharides and proteins, which are important for facilitating wound closure and remodelling processes [11].

The last two decades have witnessed a remarkable growth in research activities and applications of natural products such as propolis for healing purposes owing to their abundance in nature, diverse range of biological effects, relatively low cost and minimal side effects [12]. Propolis or bee glue is a resinous mixture produced by honeybees from materials that collected from different botanical sources (such as buds and sap) and mixed with salivary secretions. Because of its waxy character, worker bees employ it as a general-purpose sealer to coat the hive interior and fill internal cracks and crevices in the honeycombs [13]. Furthermore,

Table 1 List of classified rats based on their biomaterial treatment

Group no.	Type of treatment given
1	control
2	ZnO/W
3	ZnO/Ext
4	ZnO/Ag/Ext
5	ZnO/CuO/Ext
6	ZnO/Ag/CuO/Ext

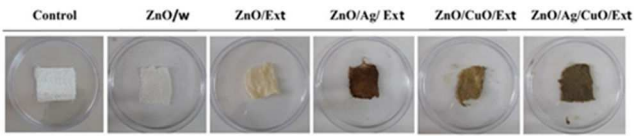

Fig. 1 *Photo of bandages after deposition of nanocomposites and control*

antimicrobial, antioxidant, antiseptic and anti-inflammatory properties of the propolis protect the hive against invaders and external contamination, preventing the bee colony from diseases. It also has been reported that chemical compounds of propolis may contribute to stimulating immune cells to synthesise cytokines that regulate smooth muscle function and tissue remodelling [14, 15].

Although the nutritional attributes and medicinal value of propolis have been well investigated in the literature, as far as we know, no study has been conducted to explore its benefits when combined with zinc oxide NPs for medicinal purposes. Towards this direction, the current research aimed at synthesising different metallic nanocomposites using propolis extract namely ZnO/W, ZnO/Ext, ZnO/Ag/Ext, ZnO/CuO/Ext and ZnO/Ag/CuO/Ext have been synthesised by microwave method and studied their potential of wound-healing activity on a rat. Characterising of NPs have done by X-ray diffraction (XRD), scanning electron microscopy (SEM), diffuse reflectance UV–visible spectroscopy (UV–vis DRS), Fourier transform infrared spectroscopy (FTIR), thermogravimetric analysis (TGA) and Brunauer–Emmett–Teller (BET) analyses. Processing of wound healing monitored by measuring the wound decreasing size and histopathological methods.

2 Experimental

2.1 Materials

The reagents involved in the present investigation were all of the analytical grades and applied without additional purification. Copper (II) acetate [$Cu(CH_3COO)_2{\cdot}H_2O$], zinc nitrate hexahydrate [$Zn(NO_3)_2{\cdot}6H_2O$], sodium hydroxide, silver nitrate [$Ag(NO_3)$] and ethanol were obtained from Merck (Darmstadt, Germany). Propolis was purchased from a domestic market (Ardabil, Iran).

2.2 Methods

2.2.1 Preparation of propolis ethanolic extract: 100 g of dried ground propolis was dissolved in 1 l of 99% ethanol by the magnetic mixer in the absence of bright for 72 h at 25°C. The resulting mixture was then filtered with filter paper. Afterwards, the solution was evaporated in a vacuum condition by rotary evaporator (45°C) and kept in the refrigerator until use [16].

2.2.2 Preparation of ZnO NPs and other nanocomposites: Briefly, 7.3 g of zinc nitrate was macerated in 100 ml of deionised water to produce ZnO/W and (6.58 g zinc nitrate), (6.58 g zinc nitrate and 0.315 g silver nitrate), (6.58 g zinc nitrate and 0.5 g copper (II) acetate) and (5.85 g zinc nitrate, 0.315 g silver nitrate and 0.5 g copper (II) acetate) were immersed in 90 ml of deionised water and then added to 10 ml of propolis extract to synthesis ZnO/Ext, ZnO/Ag/Ext, ZnO/CuO/Ext and ZnO/Ag/CuO/Ext nanocomposites, respectively. Subsequently, 5 M NaOH solution was added dropwise under vigorous stirring until the pH was adjusted to ∼10. The solutions were placed in the moderate microwave for 10 min. Then the precipitates were collected by centrifuging for 5 min at 3000 rpm and rinsed with water and ethanol to eliminate excess reagents and centrifuged again. Finally, the precipitates were kept in a stove at 65°C for 24 h to dry.

2.2.3 Characterisation: A Philips Xpert X-ray diffractometer was used to investigate the XRD patterns with a scan speed of 0.04°/s over the 2θrange of 20°–80° using Cu Kα ($\lambda = 0.15406$ nm). The particle distribution and morphology were monitored using the LEO 1430VP scanning electron microscope, at 15 kV accelerating voltage. The UV–vis DRS were obtained with a Scinco 4100 spectrophotometer. TGA of the samples was carried out with a Linseis STAPT 1000 analyser by raising the temperature in the air from room temperature to 600°C at a heating proportion of 10°C/min. The FTIR spectra were taken with a Perkin–Elmer Spectrum RX I spectrometer. The textural characteristics of the samples were studied by conducting N2 adsorption at −196°C using a Micromeritics Tristar II Plus analyser. The pH of solutions was measured using a Metrohm digital pH meter model 744.

2.2.4 In vivo study: Overall, 42 male Wistar rats, 8 weeks old and 170–190 g in weight were provided by the Experimental Animal Center at the University of Tehran. Rats were housed and fed according to standard conditions. All the experiments involving animals were carried out in compliance with the National Institutes of Health guidelines for the use and care of experimental animals (NIH Publications No. 8023, revised 1978). The rats were divided into six groups based on the applied samples and treatment approaches (Table 1). On the experiment day, the rats were anaesthetised with intraperitoneal ketamine-xylazine (3: 1, 2 ml/1 kg) and dorsal hairs were removed and the underlying skin wiped with 70% ethanol; full-thickness skin wounds (2 cm × 2 cm) were generated on the dorsum of each rat by a surgical scalpel.

2.2.5 Preparation of gauze coatings nanomaterials: Sterile gauzes were cut to 2.5 × 2.5 cm in size and immersed in a solution containing nanomaterials (20 g/100 ml) and a mixture of water: ethanol (10:1). Then, it was kept in an ultrasonic bath for 40 min at 30°C. At the end of the reaction, the colour of the dressing gauzes changed and immediately was placed on the wound (Fig. 1).

2.2.6 Histopathological studies and photographs: To evaluate the wound-healing process efficiency, monitoring all the changes during the treatment process is of vital importance. Accordingly, the wound area was traced and measured to quantify the percentage of wound closure using the following (1), [17] on days 6, 12 and 18 after wounding

$$\text{Percentageclosure}(\%) = (A_z - A_t/A_z) \times 100 \quad (1)$$

where $A_t$is the wound area on corresponding days and A_z is the wound area on day 0.

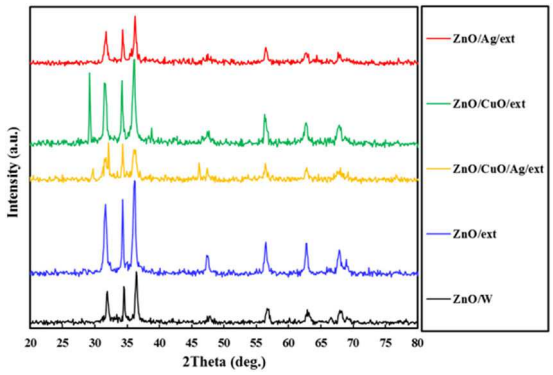

Fig. 2 *XRD patterns of the ZnO/W, ZnO/Ext, ZnO/CuO/Ext, ZnO/Ag/Ext and ZnO/Ag/CuO/Ext samples*

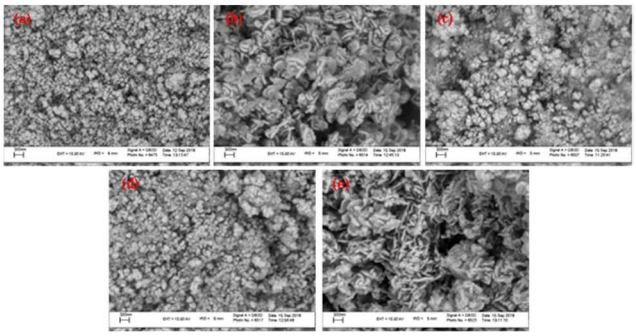

Fig. 3 *SEM images of*
(a) ZnO/W, ***(b)*** ZnO/Ext, ***(c)*** ZnO/Ag/Ext, ***(d)*** ZnO/CuO/Ext, ***(e)*** ZnO/Ag/CuO/Ext sample

2.2.7 Statistical analysis: Quantitative data of wound closure percentage were collected and expressed as average±standard error where applicable. Statistical analysis was carried out using one-way ANOVA and post hoc Tukey (SPSS) so that p-values <0.05 were regarded as significant.

3 Results and discussion

3.1 Characterisation

The crystallography of the ZnO/w, ZnO/Ext, ZnO/Ag/Ext, ZnO/CuO/Ext and ZnO/Ag/CuO/Ext samples was determined by XRD (Fig. 2). The diffraction peaks with high intensities exist at angles corresponding to (002), (004), (100), (101), (102), (103), (110), (112), (200), (201) and (202) planes revealed well crystallinity of the prepared samples. The hexagonal wurtzite structure was confirmed (JCPDS Card No. 36-3411) by the peaks in the XRD spectrum [18]. In addition, low CuO peaks and hexagonal ZnO crystal phase peaks were observed in CuO-containing nanocomposites, due to their low weight. Diffraction peaks of copper oxide are qualified for the cubical crystal phase (JCPDS Card No. 78-0428) [19]. Along with the presence of zinc oxide and copper oxide peaks in the ZnO/Ag/CuO/Ext sample, there are two low-grade Ag-based couriers. The mean crystallite size of the synthesised samples was determined using Scherrer's equation as follows:

$$D = K\lambda/\beta\cos\theta \tag{2}$$

where D is the average crystallite size (in nm), K is the Scherer's constant ($K = 0.9$), β is the corrected full-width-at half maximum (FWHM in radians) of the corresponding plane, θ is the diffraction angle ($\theta = 12.7°$) and λ is the wavelength of X-ray radiation ($\lambda =$ 0.15418 nm). The mean crystallite sizes of the ZnO/w, ZnO/Ext, ZnO/CuO/Ext, ZnO/Ag/Ext and ZnO/Ag/CuO/Ext samples calculated from the (101) plane were 19, 11.4, 21.8, 18.2 and 22.3 nm, respectively. As seen, the crystallite size of ZnO/Ag/CuO/Ext composite increased as compared to that of ZnO/w. The increase may be attributed to the simultaneous presence of ZnO, CuO and Ag in its structure. The crystallite size of ZnO/Ext and ZnO/Ag/Ext decreased compared to that of ZnO/w due to the presence of biomolecules and metabolites such as flavonoids and phenolic compounds, which are distributed in different parts of the propolis. For the observation of the surface morphology of ZnO/w, ZnO/Ext, ZnO/Ag/Ext, ZnO/CuO/Ext and ZnO/Ag/CuO/Ext samples, SEM images were captured (Fig. 3). As shown in this figure, every four nanocomposites with ZnO, have almost spherical shapes. Bio-synthesised NPs using propolis extracts (ZnO/Ext) and silver-synthesised samples (ZnO/Ag/Ext) are smaller than ZnO/w. These findings are by the outcomes of XRD patterns. This size reduction can be related to the presence of organic active compounds in the extract that attached to the surface at the time of preparation of NPs [20].

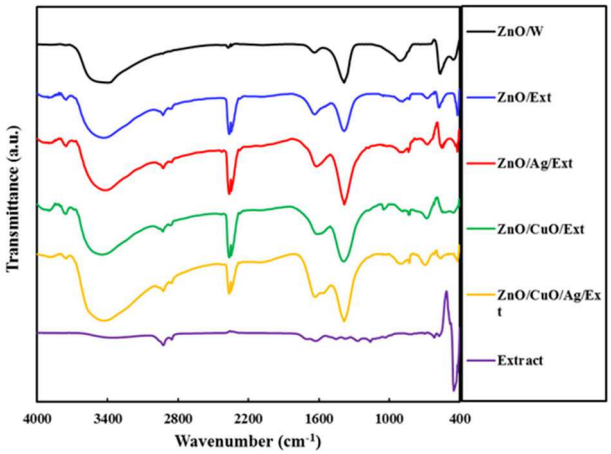

Fig. 4 *FTIR spectra for the ZnO/W, ZnO/Ext, ZnO/CuO/Ext, ZnO/Ag/Ext and ZnO/Ag/CuO/Ext samples*

FT-IR spectra of the ZnO/w, ZnO/Ext, ZnO/Ag/Ext, ZnO/CuO/Ext and ZnO/Ag/CuO/Ext specimens in the range of 400–4000 cm^{-1} are presented in Fig. 4. All the samples exhibit peaks at around 420 cm^{-1} specified to the stretching vibration Zn–O [21]. The nanocomposites ZnO/CuO/Ext and ZnO/Ag/CuO/Ext showed distinct peaks at 630 cm^{-1} corresponding to CuO [22]. Also, peaks of 890, 1020 and 1630 cm^{-1} can be connected with the stretching vibration of the C = O and C–O bonds of the biomolecules found in the propolis extract [23]. In addition, the characteristic peaks for the C–H vibrations of the CH_2 and CH_3 aliphatic was seen around 2930 cm^{-1} [24]. The FTIR spectrum of the propolis extract shows a wide peak at 3360 cm^{-1} i.e. related to the O–H group of phenolic compounds [25]. Finally, the FTIR spectra of all samples showed a wide absorption peak within range, 3400 cm^{-1}, which represents the group O–H stretching vibration [26].

Afterwards, to monitor the weight loss and thermal stability of the binded propolis extract, TGA of the samples was carried out (Fig. 5). The sample ZnO/W exhibited a losing weight of 4.6% upon inflaming to 600°C. The observed losing weight is because of the destruction and loss of adsorbed water on the stated sample. In cases of ZnO/Ext, ZnO/Ag/Ext, ZnO/CuO/Ext and ZnO/Ag/CuO/Ext samples, the losing weight due to raising the temperature up to 200°C is due to loss of water molecules; similar to ZnO/W and also OH group. However, further increases in temperature, a greater weight loss of the samples was seen, particularly in the range of 250–300°C. This temperature is typical for the decomposition of a number of organic compounds. The weight loss is related to the burning of organic biomolecules attached around the samples. The weight proportion of the biomolecules in the ZnO/Ext, ZnO/CuO/Ext, ZnO/Ag/Ext and ZnO/Ag/CuO/Ext samples have been determined 12.7, 16.8, 10 and 18.7%, correspondingly. Similar observations were recorded for TGA studies of the ZnO nanostructures prepared in the presence of various plant extracts [24].

To evaluate the electronic absorbency characteristics of the produced specimens, UV–vis DRS spectra were provided in the

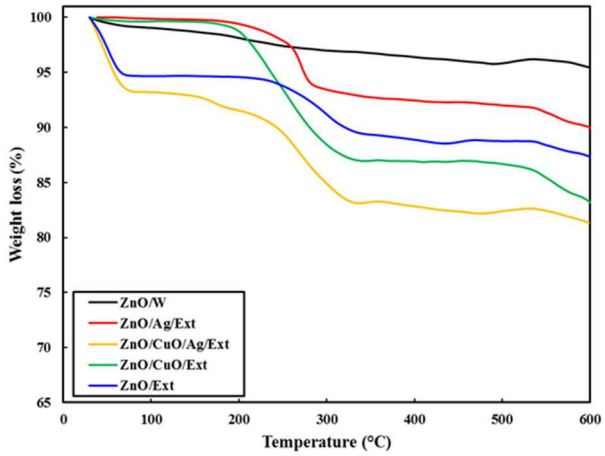

Fig. 5 *TGA curves for the ZnO/W, ZnO/Ext, ZnO/CuO/Ext, ZnO/Ag/Ext and ZnO/Ag/CuO/Ext samples*

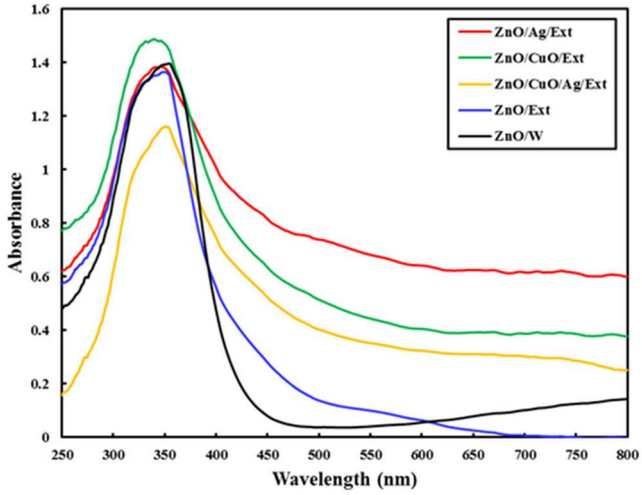

Fig. 6 *UV–vis DRS spectra of the ZnO/W, ZnO/Ext, ZnO/CuO/Ext, ZnO/Ag/Ext and ZnO/Ag/CuO/Ext samples*

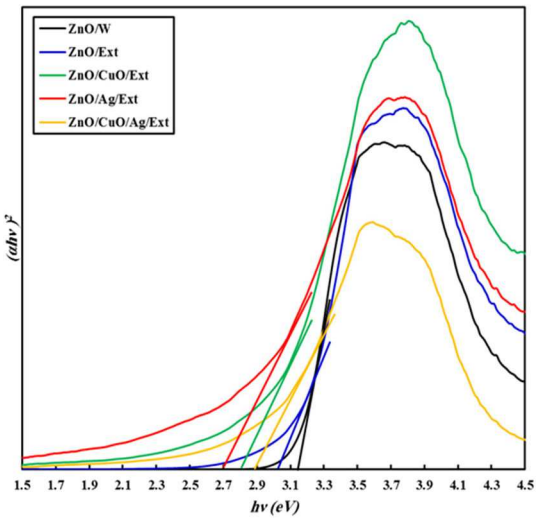

Fig. 7 *Band gaps energy curves for the ZnO/W, ZnO/Ext, ZnO/CuO/Ext, ZnO/Ag/Ext and ZnO/Ag/CuO/Ext samples*

range of 220–820 nm (Fig. 6). By the literature, the ZnO NPs synthesised in water did not absorb in the range of visible light (400–700 nm) and only exhibited an absorption peak at 360 nm in the UV region [10]. In addition, the ZnO/CuO/Ext sample exhibits a change of 20 nm in absorbance to the UV region. This change may be related to the result of the quantum bound effect. However, the other NPs synthesised in the presence of propolis extract presented a wide absorption band in visible range associated with a sharp absorption in UV wavelengths. The observed visible-light absorption can be attributed to the biomolecules of the extract attached to the NPs surface. The obtained results from the DRS data were in agreement with the FTIR spectra and TGA, indicating the presence of propolis extract biomolecules over the synthesised ZnO, ZnO/CuO, ZnO/Ag and ZnO/Ag/CuO NPs. The propolis extract is rich in bioactive components, including caffeic esters, polyphenols, flavonoids, coumaric acid, lignan and diterpene [27]. It is postulated that the phenolic compounds containing hydroxyl groups could readily chelate with Zn^{2+} ions producing complexes by a p-track conjugation effect. These complexes act as capping agents to control the growth of NPs during the synthesis process and thus tuning their size and produce more stable nanocrystals, particularly after the microwave step [21, 28].

Tauc's equation was employed to estimate the energy bandgaps (E_g) of the synthesised samples

$$ahv = B(hv - E_g)^{n/2} \tag{3}$$

where v, a and B represent the light frequency, absorption coefficient and proportionality constant, respectively [29]. The magnitude of n is dependent on the transition category in the semiconductor. The values of E_g were determined by extrapolation of the linear portion on the energy axis from the $(ahv)^2$ versus hv graphs. As shown in Fig. 7, the bandgaps of ZnO/Ext, ZnO/CuO/Ext, ZnO/Ag/Ext and ZnO/CuO/Ag/Ext nanocomposites are less than ZnO/w nanocomposites.

The measured BET surface areas and textural characteristics of the ZnO/w, ZnO/Ext, ZnO/Ag/Ext, ZnO/CuO/Ext and ZnO/CuO/Ag/Ext samples were determined by the N2 physisorption at − 196°C and the results are presented in Fig. 8. As evident in this figure, the isotherms of all samples are of type IV, indicating their mesoporous structure [30]. The calculated specific surface areas were 16.7, 19.4, 15.7, 13.3 and 21.9 m^2 g^{-1} for the ZnO/w, ZnO/Ext, ZnO/CuO/Ext, ZnO/Ag/Ext and ZnO/Ag/CuO/Ext samples, respectively. Reducing the specific surface area of nanocomposites ZnO/CuO/Ext and ZnO/Ag/Ext as compared to the ZnO/W and ZnO/Ext may be related to the blocking of active sites of the CuO- and Ag-containing particles because of the presence of certain biomolecules in biological extract or surface structure.

3.2 Rate of wound closure

The wound healing is defined as a process of repairing injured tissue to obtain restoration of integrity; whereas the wound contraction involves narrowing or closing of the wound. Accordingly to estimate the rate of closure, the wound area was measured at different time intervals. A better healing pattern of wound closure was seen in ZnO/Ag/Ext treated wounds at day 18th after wounding in comparison to the other groups ($p < 0.05$). Fig. 9 shows the wound closure rate of treated groups on different days. At first, there was a major decrease in wound size in ZnO/Ext, ZnO/CuO/Ext and ZnO/Ag/CuO/Ext treated rats on the 6th day, but the closure rate was faster in ZnO/Ext, ZnO/Ag/Ext and ZnO/Ag/CuO/Ext on subsequent days to day 12 when compared with control rats. Gauze dressing containing ZnO/CuO/Ext promoted a decrease in the wound's surface area on day 6 after application. However, based on the obtained results, there was a significant wound closure in ZnO/Ag/Ext on final days, which is probably because of zinc/silver's healing effect in the unit of time.

3.3 Histopathological examination

Re-epithelialisation is a significant stage in the healing system of skin wounds in which keratinocytes proliferate and migrate to cover the wound area and restore epidermal integrity [23]. The histopathological analyses of the skin samples demonstrated tissue re-epithelisation and cell proliferation. From the histopathological examination, as shown in Fig. 10, dermal layer formation and epidermis regeneration were initiated on 12th day in the treated

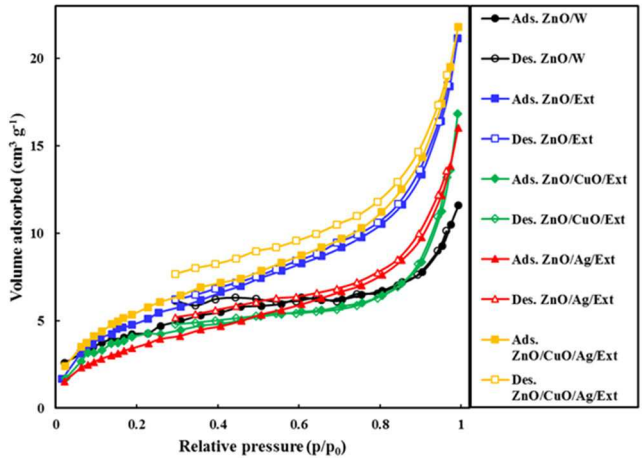

Fig. 8 *Nitrogen adsorption–desorption isotherms of the ZnO/W, ZnO/Ext, ZnO/CuO/Ext, ZnO/Ag/Ext and ZnO/Ag/CuO/Ext samples*

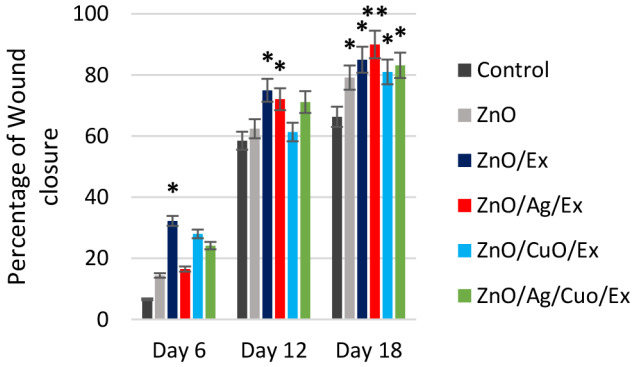

Fig. 9 *Percentage of wound closure in control and treated groups*
*The significance difference with control ($p < 0/05$). **The significance difference from all groups ($p < 0/05$)

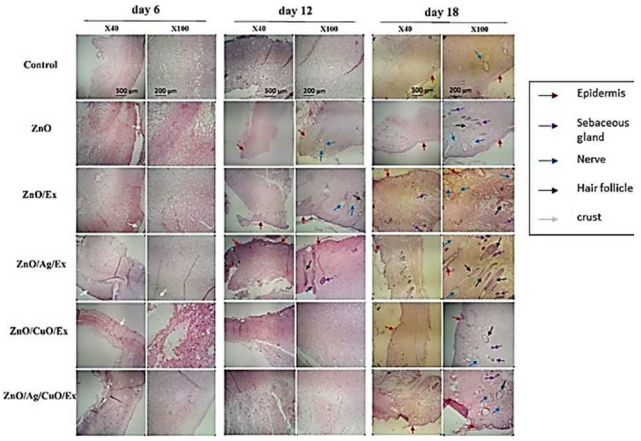

Fig. 10 *Haematoxylin and eosin staining of the wound tissues on different days of post-treatment*

samples with ZnO and ZnO/Ext. However, epidermis regeneration was completely finished on 18th day in the ZnO/Ag/Ext. On day 12, the presence of hair follicles and sebaceous glands in ZnO/Ag/Ext and hair follicles and nerves in ZnO/Ext and only nerves in ZnO were detected. However, finally, on 18th day, they clearly were improved in ZnO/Ag/Ext treated lesions as compared to the control sample. Hair follicles, which have a major role in epithelial regeneration and wound healing, can also be considered as a reservoir for the penetration of NPs inside the skin [23]. The secretion of serum proteins and cells pronounced the formation of more exuberant crusts and resulted in more efficient healing of the wounds treated with ZnO, ZnO/Ext, ZnO/CuO/Ext and particularly ZnO/Ag/Ext [31]. Moreover, the deposition of collagen in wounds was investigated by Masson's trichrome staining. As evident in

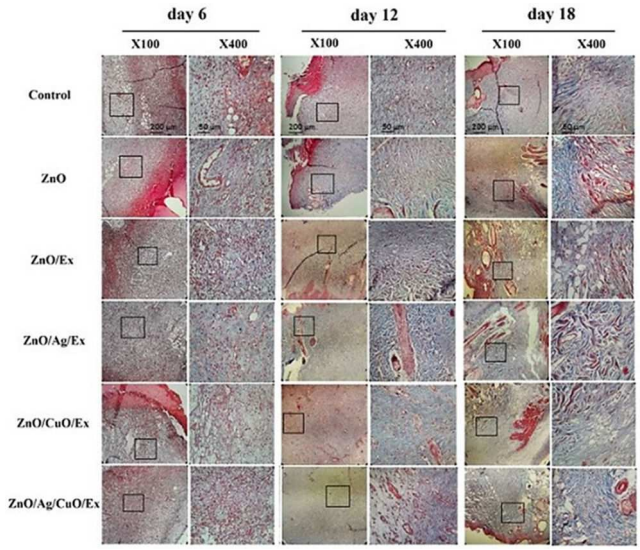

Fig. 11 *Masson's trichrome staining of wound tissues on different days of post-treatment*

Fig. 11, the wound area of control rats contains loose and disorganised collagen fibrils on the wound surface even at 18 days of post-wounding. Whereas the groups treated with ZnO, ZnO/Ext, ZnO/Ag/Ext, ZnO/CuO/Ext and ZnO/Ag/CuO/Ext demonstrated a number of dense, and ordered collagen fibrils on selected areas of each wound at 12 days of post-wounding and particularly at 18 days of post-wounding. Among the control and other groups, treatment with ZnO/Ag/Ext showed the highest disposition of collagen in the wound site on 18th day of post-treatment. In addition, penetration of skeletal muscle through to the dermal layer was observed in the wound slides of ZnO, ZnO/Ag/Ext and ZnO/CuO/Ext groups on 18th day.

It has been documented that zinc as a structural part of many proteins and enzymes that participate in cellular division, proliferation, secretion and contraction, may beneficially influence the wound healing process [32]. In this regard, studies on Dawley rats demonstrated that wounds treated with the β-chitin hydrogel/ZnO NPs bandage are associated with a decreased rate of bacterial colonies compared with that of the control, leading to a more rapid re-epithelialisation, remarkable collagen deposition and faster healing [33]. Similarly, Zhai *et al.* [34] observed that ZnO-loaded chitosan bandage could positively influence wound healing. Furthermore, the use of silver-based NPs has been well examined to reduce wound inflammation and accelerate wound healing through the regulation of cytokine [10]. Kantipudi *et al.* [27] conducted a study on the preparation of Ag–ZnO NPs and evaluated their potential as wound healing materials. They reported that in comparison with Ag NPs and standard drug, Ag–ZnO composite exhibited better performance in the wound healing process. In other work, in vivo experiments in mice demonstrated a more efficient re-epithelialisation, condensed collagen deposition and an accelerated wound healing ability of chitosan-Ag/ZnO dressings compared to the use of pure ZnO and chitosan dressing ointment gauze [9]. As mentioned earlier, due to anti-inflammatory and cell proliferation properties, propolis has been frequently used to stimulate the healing process [22, 35]. These properties are associated with the existence of a variety of biologically active compounds with therapeutic potential such as phenolic acids, flavonoids and benzoic acids, which may readily account for the perceived prophylactic effect of propolis in wound healing [15, 35, 36]. In this context, McLennan *et al.* [37] observed that the use of propolis could effectively accelerate the wound healing activity and result in re-epithelialisation of wounds in diabetic rodents. Besides, propolis provided additional benefits in reducing the infiltration of neutrophil and regulating the wound site macrophage influx. In another study, Khorasgani *et al.* [38] compared the healing rates of wounds treated with propolis against silver sulfadiazine. Based on macroscopical, microscopical and qualitative examinations, they

concluded that propolis offers a greater healing potential than other treatment method.

Therefore, in the current research, the observed wound-healing ability of ZnO/Ag/Ext gauze dressing could possibly have ascribed to the presence of ZnO and Ag, as well as synergistic effects of propolis extract, taking into account the regeneration and the presence of hair follicles, sebaceous glands and nerves was better in ZnO/Ext compared to those in ZnO/W on both the 12th and 18th days. Results showed that ZnO/Ext led to a remarkable reduction in the wound area and an increase in re-epithelialisation compared to ZnO/W gauze dressing and control sample. This action is likely due to the presence of propolis in ZnO/Ext and its medicinal properties. In addition, the potent biocidal properties of copper compounds, along with their critical role in skin regeneration and angiogenesis regulation, have led to the frequent use of copper-based complexes to promote the wound healing process [39, 40]. Similarly, Thanusha *et al.* [41] successfully synthesised hydrogel-containing CuO and ZnO NPs effective wound dressing scaffold and demonstrated its efficacy to facilitate wound healing in Wistar rats.

Overall, the healing of a wound is a multi-phase process with indistinct boundaries. Each and every element/component in the studied samples have had an impact on the healing phases, which resulted in a significant improvement in wound condition. As indicated in the results, all the samples showed significant healing effects compared to the control within 6 days of treatment, while the differences in efficiencies were insignificant with one another. Similar results were obtained from the samples on day12 of healing. However, on day 18, the differences between the studied samples were not only significant compared to control but also compared to each other. As discussed above, the differences in the healing effects could be based on the differences in their action at different stages of healing. For example, epithelium restoration around the wound area can be enhanced by ZnO. The Zn^{2+} ions released from ZnO act as a cofactor and contribute to the function of Zn-dependent matrixins [42]. Moreover, Cu takes part in various stages such as keratinocytes, remodelling of the extracellular matrix, collagen synthesis and activation of transforming growth factor-β_1 at initial stages of healing [43]. On the other hand, Ag, as a known anti-bacterial agent, also has a role in the downregulation of matrixins, when they are present at higher degrees to inhibit their negative feedback on the wound healing process [44]. Also, Ag lessens the inflammation through cytokine modulation and facilitates recovery [45]. Notably, the synergistic action of the antioxidants present in propolis should also be taken into account. Therefore, considering the several reactions involved in the wound-healing and the various roles that the employed elements/compounds play in different phases, the effectiveness of each sample has varied at day 18. Eventually, the ZnO/Ag/Ext sample had shown the highest activity for enhanced recovery of wounds.

4 Conclusion

Our findings specified that ZnO/Ag/Ext NPs hastens wound healing and upsurges wound closure ratio. A number of elements could be complicated in the improvement of the wound healing process. The company of the antioxidant, anti-inflammatory and antimicrobials properties probably among the factors that contributed to the potential wound healing effect of ZnO/Ag/Ext NPs. Additional revisions are essential to create the principal bioactive and inorganic compound accountable for the wound healing performance and the optimum conditions for the fabrication and application of ZnO/Ag/Ext NPs.

5 Acknowledgment

The authors thank the 'Clinical Research Development Center of Baqiyatallah Hospital' for their kind cooperation. The support provided by the University of Mohaghegh Ardabili was greatly appreciated.

6 References

[1] Vishwakarma, K.: 'Green synthesis of ZnO nanoparticles using abrus precatorius seeds extract and their characterization', PhD thesis, National Institute of Technology, Rourkela, 2013

[2] Mohan, Y.M., Lee, K., Premkumar, T., *et al.*: 'Hydrogel networks as nanoreactors: a novel approach to silver nanoparticles for anti-bacterial applications', *Polymer*, 2007, **48**, pp. 158–164

[3] Patil, P.S., Fountas-Davis, N., Huang, H., *et al.*: 'Fluorinated methacrylamide chitosan hydrogels enhance collagen synthesis in wound healing through increased oxygen availability', *Acta Biomater.*, 2016, **36**, pp. 164–174

[4] Gong, C., Wu, Q., Wang, Y., *et al.*: 'A biodegradable hydrogel system containing curcumin encapsulated in micelles for cutaneous wound healing', *Biomaterials*, 2013, **34**, (27), pp. 6377–6387

[5] Alborova, A., Lademann, J., Meye, L., *et al.*: '*Application of laser scanning microscopy for the characterization of wound healing*' (GMS Krankenhaushygiene Interdisziplinär, Switzerland, 2007), **2**, p. 37

[6] Fan, X., Zheng, Y.: 'Biosynthesis of eco-friendly and recyclable Pd/LDHs catalyst using the withered leaves extract for Suzuki coupling reaction', *IET Nanobiotechnol.*, 2020, **14**, (1), pp. 59–65

[7] Giménez, V.M.M., Russo, M.G., Narda, G.E., *et al.*: 'Synthesis, physicochemical characterisation and biological activity of anandamide/ε-polycaprolactone nanoparticles obtained by electrospraying', *IET Nanobiotechnol.*, 2020, **14**, (1), pp. 86–93

[8] Bayrami, A., Alioghli, S., Pouran, S.R., *et al.*: 'A facile ultrasonic-aided biosynthesis of ZnO nanoparticles using *Vaccinium arctostaphylos* L. leaf extract and its antidiabetic, anti-bacterial, and oxidative activity evaluation', *Ultrason. Sonochem.*, 2019, **55**, pp. 57–66

[9] Lu, Z., Gao, J., He, Q., *et al.*: 'Enhanced anti-bacterial and wound healing activities of microporous chitosan-Ag/ZnO composite dressing', *Carbohydr. Polym.*, 2017, **156**, pp. 460–469

[10] Tian, J., Wong, K.K., Ho, C.M., *et al.*: 'Topical delivery of silver nanoparticles promotes wound healing', *ChemMedChem*, 2007, **2**, (1), pp. 129–136

[11] Borkow, G., Gabbay, J., Zatcoff, R.C.: 'Could chronic wounds not heal due to too low local copper levels?', *Med. Hypotheses*, 2008, **70**, (3), pp. 610–613

[12] Bayrami, A., Ghorbani, E., Pouran, S.R., *et al.*: 'Enriched zinc oxide nanoparticles by *Nasturtium officinale* leaf extract: joint ultrasound-microwave-facilitated synthesis, characterization, and implementation for diabetes control and bacterial inhibition', *Ultrason. Sonochem.*, 2019, **58**, p. 104613

[13] Castaldo, S., Capasso, F.: 'Propolis, an old remedy used in modern medicine', *Fitoterapia*, 2002, **73**(Suppl 1), pp. S1–S6

[14] Bonvehí, J.S., Coll, F.V., Jordà, R.E.: 'The composition, active components and bacteriostatic activity of propolis in dietetics', *J. Am. Oil Chem. Soc.*, 1994, **71**, (5), pp. 529–532

[15] Moreno, M.I.N., Isla, M.I., Sampietro, A.R., *et al.*: 'Comparison of the free radical-scavenging activity of propolis from several regions of Argentina', *J. Ethnopharmacol.*, 2000, **71**, (1–2), pp. 109–114

[16] Abdelaal, A., Abozid, M.: 'Chemical composition of Egyptian and commercial propolis and its effects on liver function and lipid profiles in albino rats', *J. Biological Chem. Env. Res.*, 2013, **8**, pp. 323–340

[17] Raghuwanshi, N., Kumari, P., Srivastava, A.K., *et al.*: 'Synergistic effects of *Woodfordia fruticosa* gold nanoparticles in preventing microbial adhesion and accelerating wound healing in Wistar albino rats in vivo', *Mater. Sci. Eng. C. Mater. Biol. Appl.*, 2017, **80**, pp. 252–262

[18] Mohammadi-Aloucheh, R., Habibi-Yangjeh, A., Bayrami, A., *et al.*: 'Enhanced anti-bacterial activities of ZnO nanoparticles and ZnO/CuO nanocomposites synthesized using *Vaccinium arctostaphylos* L. fruit extract', *Artif. Cells Nanomed. Biotechnol.*, 2018, **46**, pp. 1200–1209

[19] Kuznetsov, M.V., Mafina, M.K., Belousova, O.V., *et al.*: 'Catalytically active magnetic nanoparticles in the Cu-O system', *Inorg. Mater.*, 2015, **51**, (4), pp. 307–318

[20] Mohammadi-Aloucheh, R., Habibi-Yangjeh, A., Bayrami, A., *et al.*: 'Green synthesis of ZnO and ZnO/CuO nanocomposites in *Mentha longifolia* leaf extract: characterization and their application as anti-bacterial agents', *J. Mater. Sci., Mater. Electron.*, 2018, **29**, (16), pp. 13596–13605

[21] Bayrami, A., Parvinroo, S., Habibi-Yangjeh, A., *et al.*: 'Bio-extract-mediated ZnO nanoparticles: microwave-assisted synthesis, characterization and antidiabetic activity evaluation', *Artif. Cells Nanomed. Biotechnol.*, 2018, **46**, (4), pp. 730–739

[22] Sharaf, S., Higazy, A., Hebeish, A.: 'Propolis induced anti-bacterial activity and other technical properties of cotton textiles', *Int. J. Biol. Macromol.*, 2013, **59**, pp. 408–416

[23] Ito, M., Liu, Y., Yang, Z., *et al.*: 'Stem cells in the hair follicle bulge contribute to wound repair but not to homeostasis of the epidermis', *Nat. Med.*, 2005, **11**, (12), pp. 1351–1354

[24] Arvanag, F.M., Bayrami, A., Habibi-Yangjeh, A., *et al.*: 'A comprehensive study on antidiabetic and anti-bacterial activities of ZnO nanoparticles biosynthesized using *Silybum marianum* L seed extract', *Mater. Sci. Eng., C*, 2019, **97**, pp. 397–405

[25] Azevedo, L.F., Priscilla da Fonseca, S., Brandão, M.P., *et al.*: 'Polymeric nanoparticle systems loaded with red propolis extract: a comparative study of the encapsulating systems, PCL-pluronic versus Eudragit®E100-pluronic', *J. Apic. Res.*, 2018, **57**, (2), pp. 255–270

[26] Javed, R., Ahmed, M., ul Haq, I., *et al.*: 'PVP and PEG doped CuO nanoparticles are more biologically active: anti-bacterial, antioxidant, antidiabetic and cytotoxic perspective', *Mater. Sci. Eng. C. Mater. Biol. Appl.*, 2017, **79**, pp. 108–115

[27] Kantipudi, S., Sunkara, J.R., Rallabhandi, M., *et al.*: 'Enhanced wound healing activity of Ag–ZnO composite NPs in Wistar albino rats', *IET Nanobiotechnol.*, 2018, **12**, (4), pp. 473–478
[28] Velmurugan, P., Park, J.H., Lee, S.M., *et al.*: 'Eco-friendly approach towards green synthesis of zinc oxide nanocrystals and its potential applications', *Artif. Cells Nanomed. Biotechnol.*, 2016, **44**, (6), pp. 1537–1543
[29] Feizpoor, S., Habibi-Yangjeh, A., Vadivel, S.: 'Novel TiO_2/Ag_2CrO_4 nanocomposites: efficient visible-light-driven photocatalysts with n–n heterojunctions', *J. Photochem. Photobiol. A*, 2017, **341**, pp. 57–68
[30] Pirhashemi, M., Habibi-Yangjeh, A., Pouran, S.R.: 'Review on the criteria anticipated for the fabrication of highly efficient ZnO-based visible-light-driven photocatalysts', *J. Ind. Eng. Chem.*, 2018, **62**, pp. 1–25
[31] Cahú, T.B., Silva, R.A., Silva, R.P., *et al.*: 'Evaluation of chitosan-based films containing gelatin, chondroitin 4-sulfate and ZnO for wound healing', *Appl. Biochem. Biotechnol.*, 2017, **183**, (3), pp. 765–777
[32] Lansdown, A.B., Mirastschijski, U., Stubbs, N., *et al.*: 'Zinc in wound healing: theoretical, experimental, and clinical aspects', *Wound Repair. Regen.*, 2007, **15**, (1), pp. 2–16
[33] Kumar, P.T.S., Lakshmanan, V.-K., Raj, M., *et al.*: 'Evaluation of wound healing potential of beta-chitin hydrogel/nano zinc oxide composite bandage', *Pharm. Res.*, 2013, **30**, (2), pp. 523–537
[34] Zhai, M., Xu, Y., Zhou, B., *et al.*: 'Keratin-chitosan/n-ZnO nanocomposite hydrogel for antimicrobial treatment of burn wound healing: characterization and biomedical application', *J. Photochem. Photobiol., B*, 2018, **180**, pp. 253–258
[35] Blonska, M., Bronikowska, J., Pietsz, G., *et al.*: 'Effects of ethanol extract of propolis (EEP) and its flavones on inducible gene expression in J774A.1 macrophages', *J. Ethnopharmacol.*, 2004, **91**, (1), pp. 25–30
[36] Iyyam Pillai, S., Palsamy, P., Subramanian, S., *et al.*: 'Wound healing properties of Indian propolis studied on excision wound-induced rats', *Pharm. Biol.*, 2010, **48**, (11), pp. 1198–1206
[37] McLennan, S.V., Bonner, J., Milne, S., *et al.*: 'The anti-inflammatory agent propolis improves wound healing in a rodent model of experimental diabetes', *Wound Repair. Regen.*, 2008, **16**, (5), pp. 706–713
[38] Khorasgani, E.M., Karimi, A.H., Nazem, M.R.: 'Comparison of healing effects of propolis and silver sulfadiazine on full thickness skin wounds in rats', *Pak Vet. J.*, 2010, **30**, (2), pp. 72–74
[39] Rakhmetova, A.A., Alekseeva, T.P., Bogoslovskaya, O.A., *et al.*: 'Wound-healing properties of copper nanoparticles as a function of physicochemical parameters', *Nanotechnol. Russ.*, 2010, **5**, (3), pp. 271–276
[40] Borkow, G., Gabbay, J.: 'Copper as a biocidal tool', *CurrMedChem*, 2005, **12**, (18), pp. 2163–2175
[41] Thanusha, A.V., Dinda, A.K., Koul, V.: 'Evaluation of nano hydrogel composite based on gelatin/HA/CS suffused with asiatic acid/Zno and Cuo nanoparticles for second degree burns', *Mater. Sci. Eng. C Mater. Biol. Appl.*, 2018, **89**, pp. 378–386
[42] Martins, V.L., Caley, M., O'Toole, E.A.: 'Matrix metalloproteinases and epidermal wound repair', *Cell Tissue Res.*, 2013, **351**, pp. 255–268
[43] Gopal, A., Kant, V., Gopalakrishnan, A., *et al.*: 'Chitosan-based copper nanocomposite accelerates healing in excision wound model in rats', *Eur. J. Pharmacol.*, 2014, **731**, pp. 8–19
[44] Atiyeh, B.S., Costagliola, M., Hayek, S.N., *et al.*: 'Effect of silver on burn wound infection control and healing: review of the literature', *Burns*, 2007, **33**, (2), pp. 139–148
[45] Borkow, G., Gabbay, J., Dardik, R., *et al.*: 'Molecular mechanisms of enhanced wound healing by copper oxide-impregnated dressings', *Wound Repair. Regen.*, 2010, **18**, (2), pp. 266–275